Vol 8 No 2 (2026) *e*-ISSN: 2682-8383

Journal of Engineering Technology and Applied Physics

Electrical Performance of Zn–Cu Plant-Based Cells in Aloe Vera: Leaf-Stem Comparison with Series and Parallel Scaling

Sk Rakibur Rahman[1], Eng Eng Ngu1[1, 2], Gwo Chin Chung[1], Wai Leong Pang[3], Kar Ban Tan[4], Muhammad Aqeel Ashraf[1], Ajay Kumar Singh[5] and Kah Yoong Chan[1, 6, *]

[1]*Faculty of Artificial Intelligence and Engineering, Multimedia University, Persiaran Multimedia, 63100, Cyberjaya, Selangor, Malaysia.*

[2]*Centre for Electric Energy and High Voltage Engineering, COE for Robotics and Sensing Technologies, Multimedia University, Persiaran Multimedia, 63100, Cyberjaya, Selangor, Malaysia.*

[3]*School of Engineering, , Faculty of Innovation & Technology, Taylor's University, 47500 Subang Jaya, Selangor, Malaysia.*

[4]*Department of Chemistry, Faculty of Science, Universiti Putra Malaysia, 43400 Serdang, Selangor, Malaysia.*

[5]*Faculty of Electronics and Communication Engineering, NIIT University, Rajasthan, India.*

[6]*Centre for Advanced Devices and Systems, COE for Robotics and Sensing Technologies, Multimedia University, Persiaran Multimedia, 63100, Cyberjaya, Selangor, Malaysia.*

[*]*Corresponding author*: kychan@mmu.edu.my, *ORCiD*: 0000-0003-1076-5034

https://doi.org/10.33093/jetap.2026.8.2.20

Manuscript Received: 9 February 2026, Revised: 10 March 2026, Accepted: 15 March 2026, Published: 15 September 2026

***Abstract*—Plant tissue may act as a weak electrochemical battery when electrodes of various metals are introduced. However, leaf-based systems typically experience local damage and drying around the insertion site, raising questions regarding long-term usage. A single *Aloe vera* plant was treated with a *Zn-Cu* electrode pair on a mature leaf and stem. Based on our accepted conference study's optimum leaf orientation, leaf measurements were taken horizontally along the leaf's length direction. In stem testing, horizontal positioning yielded greater current and lower effective resistance than vertical placement. The leaf and stem generated equivalent open-circuit voltages of 0.958 V and 0.943 V and short-circuit currents of 0.15 mA and 0.12 mA in a horizontal arrangement. Scaling was evaluated by combining one horizontal leaf cell and one horizontal stem cell. The obtained voltage from the series connection was 1.883 V, while the obtained current was 0.25 mA from the parallel connection. An effective resistance calculation and a simple equivalent-source model were used to verify the expected circuit behaviour. After seven days, the leaf insertion site exhibited degradation, whereas the stem site remained reasonably intact, indicating that stem implantation may retain a similar yield with enhanced durability for longer-term harvesting.**

Keywords*—PBC, Aloe vera, Leaf–stem comparison, Equivalent circuit modelling, Internal resistance.

I. INTRODUCTION

Commercially available sensing and monitoring systems are increasingly being integrated into agricultural, architectural, and outdoor environments. A significant number of these nodes continue to depend on batteries, resulting in maintenance as an implicit cost. Energy harvesting techniques are extensively employed to minimize battery usage and enhance the sustainability of wireless sensor networks [1]. However, a single source is seldom flawless and under all weather conditions. Investigations into alternatives, such as radiative cooling-based electricity generation, highlight the significance of complementary sources beyond daytime solar energy [2 - 4].

Numerous opportunities exist for harvesting. Research has been conducted on photovoltaics, vibration, thermal gradients, and ambient RF in the context of low-power electronics [1]. The issue arises from the intermittent and site-specific nature of many sources, resulting in harvested power being significantly influenced by environmental and locational factors [1, 2]. This prompts an

Published by MMU PRESS. URL: https://journals.mmupress.com/index.php/jetap/index

investigation into sources related to the sensing problem, rather than focusing on the destination, such as living plants in agriculture and green infrastructure.

Living plants may function as decentralized, low-energy power sources at the specific sites where sensing is required. Electricity generation in plant microbial fuel cells can be sustained due to the continuous supply of organic compounds to the root zone during plant growth [5, 6]. Demonstrations, such as utilizing electricity generated by living plants to operate a small radio transmitter, suggest that plant-based bioelectricity is capable of powering actual electronic devices when the power is effectively managed [7]. Recent reviews indicate that the harvesting of living plants holds potential for smart agriculture and sensing fields; however, practical constraints in deployment continue to impede widespread adoption [8].

The primary focus of this discussion is plant-based cells (PBCs). PBCs are fundamentally grounded in the electrochemical processes occurring within plant tissue. When two distinct metals are inserted into a conductive plant substrate, the fluids within the plant act as an electrolyte, potentially generating a small voltage between the two metals [9]. *Aloe vera*-derived plant cells have been examined using *Zn-Cu* electrode pairs, along with basic repeat units arranged in both series and parallel configurations [10, 11].

Prior studies on PBC have predominantly focused on leaf-based designs and electrical scaling methods. A systematic study of electrode materials, spacing, pair numbers, and connection methods (series or parallel) for aloe leaves has been documented [12]. Subsequent studies have shown the efficacy of integrating aloe-derived plant cells with power management systems to activate wireless devices for remote sensor illumination [10]. In addition to aloe, other plants, notably Opuntia, demonstrate bio-battery-style demonstrations, suggesting wider applicability in on-site [12]. Additionally, concepts associated with plant energy have been investigated, encompassing conversion processes related to plant surfaces and biointerfacing [13], alongside direct photo-driven bioelectrochemical conversion in living plants [14]. Our previous conference work advances the PBC line of inquiry and examines essential factors for optimization [15], and our other work develops the electrode material composition for sustainability [16].

Current research on *Aloe vera*-based bio-cellular materials primarily focuses on enhancing short-term electrical energy yield through modifications in electrode materials, spacing, and wiring configurations, with the leaf continuing to serve as the standard testing site [11]. The loss of sap during leaf insertion may reduce conductivity over time [11]. While energy harvesting demonstrates high efficiency during peak performance, evaluations of living plants consistently highlight challenges related to aging and scalability [8]. The prolonged use of systems like PBC, which necessitate consistent performance and electrode integrity, underscores the importance of durability and longevity for effective operation in practical applications [8, 10, 11].

This study examines a *Zn-Cu* electrode pair with a 1 cm gap, optimized in our earlier work [15], inserted in the aloe leaf and stem. Electrodes were oriented differently. Our accepted conference research recommended horizontal (along the leaf length) leaf measurements [17]. Measurements for the stem were taken both horizontally and vertically (across leaf width). In a basic circuit, measurable voltage and current were utilized to compute effective internal resistance. The optimized pair in the stem and the horizontally inserted pair in the leaf are interconnected in series and parallel following optimized alignment. Electrical outputs are assessed in relation to observable tissue changes after seven days to ensure stability and practical deployability. Section II describes the materials and methods, Section III presents results and discussion, and Section IV concludes the paper.

II. MATERIALS AND METHODS

This section provides a detailed description of the plant sample, the electrode fabrication, the placement schemes, the measurement protocol, and the data processing procedures.

A. Plant Specimen and Test Location

Experiments were conducted using a single potted *Aloe vera* plant. The plant was of indeterminate age. A single mature leaf, about 27 cm in length, was picked among the available leaves, as depicted in Fig. 1. The stem measurement was taken above the ground, at the lowest leaf zone, on the exposed section of the stem.

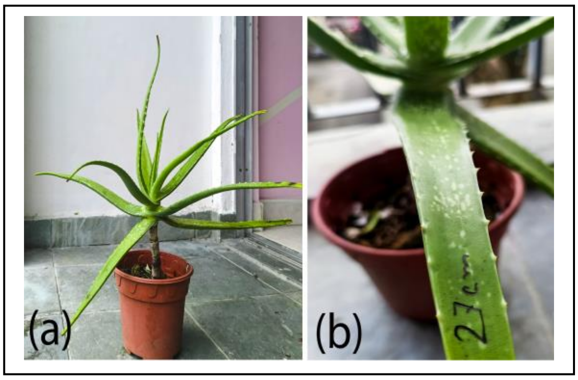

Fig. 1. (a) *Aloe Vera* plant and (b) Selected leaf size.

All trials were conducted on a residential balcony with partial exposure to both indoor and outdoor environments. At 1:15 PM (daytime).

B. Electrode Materials and Surface Preparation

A pair of metal electrodes of zinc (*Zn*) and copper (*Cu*) was chosen. All electrodes were rectangular plates that were 2.0 cm in length and 1.25 cm in width, as illustrated in Fig. 2(a) and Fig. 2(b), respectively. Before inserting any of the electrodes, they were cleaned using a swab soaked in 70% isopropyl alcohol.

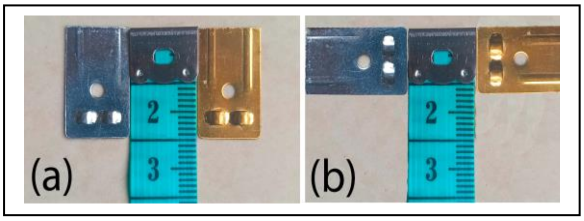

Fig. 2. (a) Zn-Cu Electrode pair length and (b) Zn-Cu Electrode pair width.

C. *Electrode Placement Geometry and Orientations*

The electrodes were inserted into the plant tissue to a depth of about 0.75 cm. The distance from base to base between the *Zn* and *Cu* electrodes was set at 1 cm.

Fig. 3. (a) Electrodes horizontally placed in the leaf, (b) Electrodes horizontally placed in the stem and (c) Electrodes vertically placed in the stem.

Two distinct orientations were tested. The *Zn-Cu* pair was positioned horizontally according to the length of the stem or leaf. The alternate pair was organized vertically according to the stem's breadth. Figure 3 illustrates the orientations.

Electrodes were inserted once at the designated location for each configuration. The multimeter probes were subsequently applied to the exposed electrode tabs. The same insertion holes were utilized when transitioning between voltage and current measurements. Electrodes were removed after measurement.

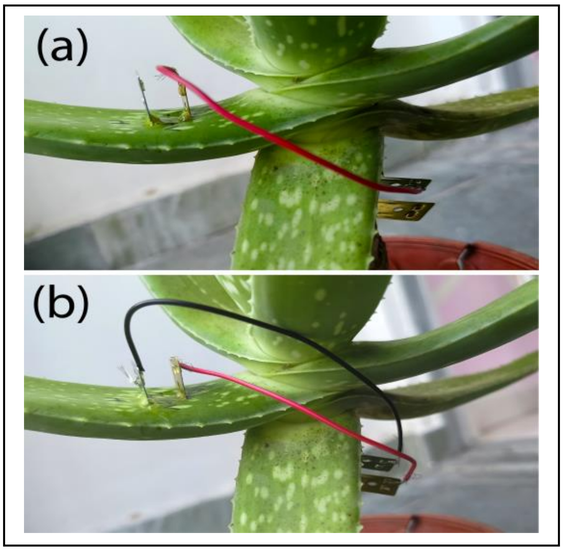

Fig. 4. (a) Series connection and (b) Parallel connection.

To assess basic scalability, one horizontal pair in the stem and one horizontal pair in the leaf were interconnected using two wiring configurations.

1. *The series connection* involved measuring the free terminal voltage across the two outer terminals after the joining of the inner terminals, as illustrated in Fig. 4(a).
2. *The parallel connection* was established by connecting both positive terminals and both negative terminals, with the combined output measured across the common nodes, as illustrated in Fig. 4(b).

D. *Electrical Measurement Procedure*

Electrical measurements were carried out using an OWON B33+ digital multimeter. Measurements of open-circuit voltage (V_{oc}) were performed in DC voltage mode, with probes directly connected via crocodile clips to the Cu and Zn electrodes, without the incorporation of external resistance.

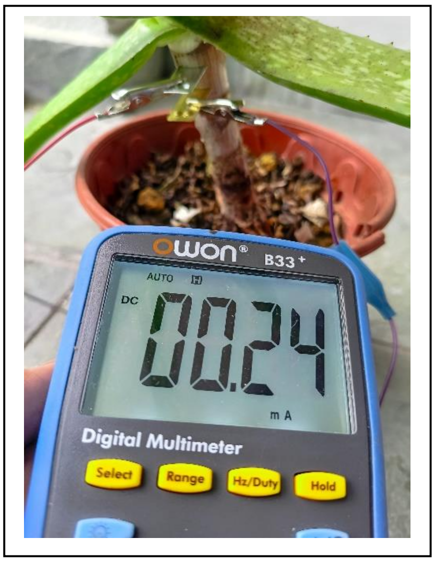

Fig. 5. Measuring V_{oc} and I_{sc} using a multimeter.

The short-circuit current (I_{sc}) was measured in DC mode, as illustrated in Fig. 5, with the meter positioned across the two electrodes. The measured current was subsequently routed through the meter's internal shunt. The settling time was permitted to be 2 minutes following the insertion of the electrodes. Each condition was assessed with a single reading.

E. *Environmental and Soil Condition Logging*

Ambient parameters were recorded using a Xiaomi Mijia Smart Thermometer 3, and soil parameters were recorded using an Avosky Soil Survey Analyzer during the measurement period. Ambient temperature was 31.8 °C, and relative humidity was 65%. Soil pH was 7. This neutral soil had a temperature of 32 °C. Soil moisture was recorded as WET+. Sunlight intensity was recorded as LOW+, as illustrated in Fig. 6.

The analyzer reports sunlight intensity using nine levels (LOW- to HIGH+). It reports moisture using five levels (DRY+ to WET+). The instrument labels were used as recorded.

Fig. 6. Ambient and Soil parameters measuring tools.

F. Data Processing and Effective Resistance Estimation

Electrical power was calculated from measured voltage and current using:

$$P = V \times I \tag{1}$$

Power is reported in milliwatts (mW).

R_{eff} is used to quantify the difficulty of current delivery by the plant-based cell under each configuration.

$$R_{eff} = \frac{Voc}{Isc} \tag{2}$$

, where V_{oc} stands for the voltage under open circuit conditions, and I_{sc} stands for the short circuit current. This equation gives a calculated value, which is not necessarily a known value, making it easy to compare the degrees of internal losses for different positions. Results are represented in kilohms (kΩ).

Short-circuit current (I_{sc}) is read in current mode by adjusting the unit in the multimeter display. Thus, resistance is also measured as an effective value.

G. Seven-day Visual Record

A qualitative visual documentation of tissue response was obtained utilizing a phone camera. Images were captured on the measurement day (day 0) and subsequently after seven days (day 7). Following the electrical measurements, the electrodes were removed.

Table I. Test matrix and measured quantities.

Test ID	Tissue	Orientation	Connection	Recorded quantities
T1	Leaf	Horizontal	Single pair	V_{oc}, I_{sc}
T2	Stem	Horizontal	Single pair	V_{oc}, I_{sc}
T3	Stem	Vertical	Single pair	V_{oc}, I_{sc}
T4	Leaf + Stem	Horizontal	Series	V_{oc}, I_{sc}
T5	Leaf + Stem	Horizontal	Parallel	V_{oc}, I_{sc}

Table I presents a summary of the experimental test matrix employed in this study. The document enumerates the tissue location, electrode orientation, and connection type assessed, in addition to the electrical quantities recorded for each instance (V_{oc} and I_{sc}).

III. RESULTS AND DISCUSSION

This section outlines the measured electrical outputs for each configuration and analyzes the primary trends related to tissue location, electrode orientation, and series–parallel scaling.

Table II presents a summary of the measured V_{oc} and I_{sc} for all cases, as well as the derived parameters utilized in the discussion.

Table II. Measured electrical output and derived parameters for each configuration.

Test ID	Configurations	V_{oc} (V)	I_{sc} (mA)	R_{eff} (kΩ)	P (mW)
T1	Leaf-H	0.958	0.15	6.39	0.14370
T2	Stem-H	0.943	0.12	7.86	0.11316
T3	Stem-V	0.904	0.04	22.60	0.03616
T4	Series (Leaf-H + Stem-H)	1.883	0.13	14.48	0.24479
T5	Parallel (Leaf-H ‖ Stem-H)	0.908	0.25	3.63	0.22700

A. Open-circuit Voltage (V_{oc})

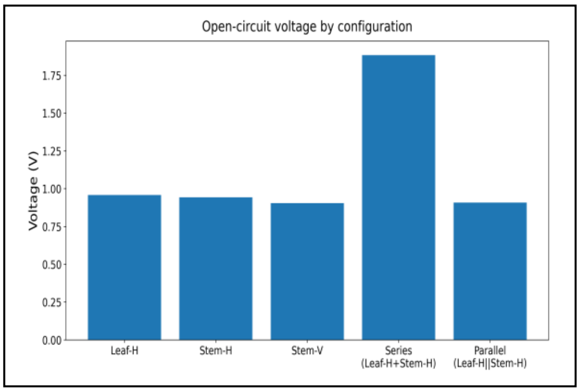

Fig. 7. Open-circuit voltage by configuration.

Figure 7 presents the values of open-circuit voltage. The individual pair voltages approximate 1 V and exhibit considerable stability [10, 11]. The Leaf-H and Stem-H configurations exhibit similarities, suggesting that the tissue location does not significantly affect the voltage level, given the same zinc-copper pair. Transitioning from a horizontal to a vertical orientation in the stem results in a minor reduction in voltage. The most significant alteration occurs during the scaling process. The voltage in a series combination reaches up to 1.88 V, whereas the parallel configuration approximates the voltage of a single cell.

B. Short-circuit Current (I_{sc})

Figure 8 presents a summary of the short circuit current results. The current changes significantly more than the voltage. The Leaf-H and Stem-H values remain constant, while the stem vertical case exhibits a significant change to 0.04 mA. Previous studies have also reported that current extraction in plant-based cells can vary significantly depending on electrode placement and tissue orientation [11]. This suggests that the direction of the stem significantly affects current extraction, even when the voltage remains comparable. The scaled results indicate that the highest current, approximately 0.25 mA, occurs when the connections are configured in parallel. In contrast, the series connection preserves the current in a manner analogous to the single pair measurements.

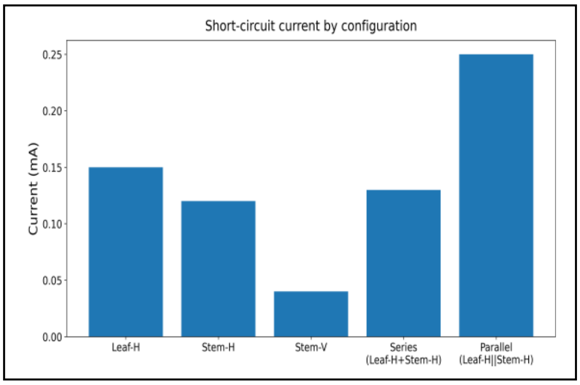

Fig. 8. Short-circuit current by configuration.

C. *Effective Resistance Estimate (R_{eff})*

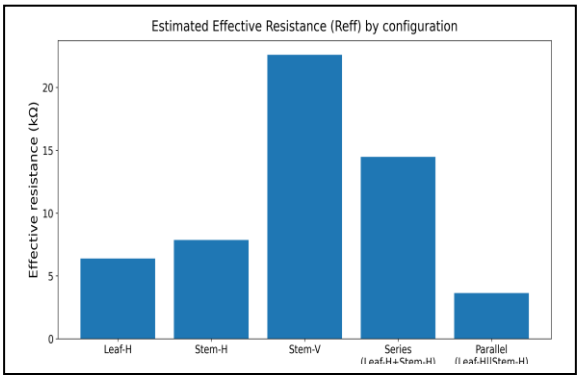

Fig. 9. Estimated effective resistance by configuration.

Figure 9 shows the result of the effective resistance calculation, $R_{eff} = V_{oc} / I_{sc}$, defined as the ratio between the open-circuit voltage and the short-circuit current. This figure clarifies why some configurations have equal voltage levels while showing very different current levels. It is noteworthy that Stem-V exhibits the highest effective resistance, which corresponds to the lowest current delivery among the tested configurations. Stem-H exhibits a significantly lower value, analogous to the findings for Leaf-H. Internal resistance has frequently been identified as a major limiting factor in plant-based electrical harvesting systems [7]. The scaling configuration aligns with the anticipated outcomes. The series configuration exhibits a higher resistance level than the individual results of the horizontal leaf cell, whereas the parallel configuration demonstrates the lowest resistance level.

D. *Power Index ($P=V_{oc} \times I_{sc}$)*

Figure 10 displays the estimated power of the various configurations considered in this study. The power values were derived from the open circuit voltage and short circuit current values. For the single-pair cases, Leaf-H yields the maximum power, then Stem-H for the horizontal leaf and stem configurations, respectively. The vertical stem configuration (Stem-V) produces the lowest power, which is mainly due to its much smaller current value. When two cells are combined, the series connection gives the highest power among all configurations because the voltages of the two cells add together, which is consistent with the expected behaviour of series-connected electrochemical cells [10, 11]. The parallel connection also increases the output compared with the individual cells, mainly due to the higher current, although its power remains slightly lower than that of the series configuration.

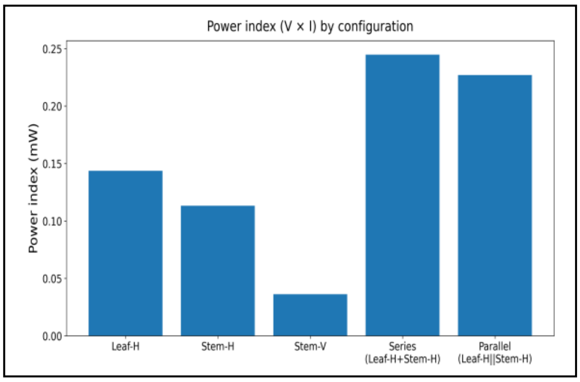

Fig. 10. Calculated power by configuration.

In order to verify the consistency of results, the measurements were repeated under analogous conditions with the same setup. The results of the repeated measurements are compared with the original data in Table III. The power variation is seen to be quite small, and it is between approximately 0.6% and 2.5% for all the configurations.

Table III. Comparison of original and repeated power values with percentage variation.

Test ID	Original *P* (mW)	Repeated *P* (mW)	Variation (%)
T1	0.14370	0.14206	1.14
T2	0.11316	0.11600	2.51
T3	0.03616	0.03592	0.66
T4	0.24479	0.24282	0.80
T5	0.22700	0.22988	1.27

These slight differences are to be expected as minor variations in the contact of electrodes and the conditions of the individual plants can influence the readings. Although there are small differences, the general trend is the same, and that would indicate the measurements are fairly consistent in that respect.

E. *Simple Internal-resistance Model and Simulation Check*

A simple equivalent circuit model as shown in Fig. 11, can aid in relating the data to engineering design. Each plant-based cell can be viewed as a source with V_{oc} in series with an internal resistance. A first estimate can be obtained using the data as follows:

$$R_{eff} \approx \frac{Voc}{Isc} \quad (3)$$

This value is considered an estimate of effective resistance under the specified measurement conditions. The internal resistance is reiterated in the evaluations of plant energy as a constraining factor, as it dictates the amount of current that can be extracted [7]. This can elucidate the significant disparities between the two cases with comparable voltage values.

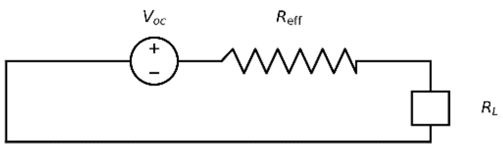

Fig. 11. Equivalent-source model used for analysis.

The data derived from the horizontal single pair scenario facilitates the model's prediction of series and parallel operations. In a series configuration, resistances are additive, whereas in a parallel configuration, the overall resistance is reduced. The results can be compared with the obtained values. The resistance values exhibit similarities, while the voltage values are comparatively close.

In this paper, V_1, R_1 and V_2, R_2 denote the V_{oc} and R_{eff} values of the two individual horizontal cells (leaf-H and stem-H). For a series connection,

$$V_{oc,\,ser} = V_1 + V_2 \tag{4}$$

$$R_{series} = R_1 + R_2 \tag{5}$$

For parallel connection,

$$R_{parallel} = \left(\frac{1}{R_1} + \frac{1}{R_2}\right)^{-1} \tag{6}$$

$$V_{oc,parallel} = \frac{\left(\frac{V_1}{R_1} + \frac{V_2}{R_2}\right)}{\left(\frac{1}{R_1} + \frac{1}{R_2}\right)} \tag{7}$$

Table IV. Predicted versus measured series/parallel results using the single-pair equivalent model.

Quantity	Predicted	Measured	Error (%)
Series V_{oc} (V)	1.901	1.883	−0.95
Series R_{eff} (kΩ)	14.25	14.48	+1.68
Parallel V_{oc} (V)	0.951	0.908	−4.52
Parallel R_{eff} (kΩ)	3.52	3.63	+3.18

The comparison between predicted and measured values using the equivalent model is summarized in Table IV. The minor voltage difference observed when cells are connected in parallel can be readily elucidated. Plant cells are not effective as voltage supplies. Certain factors, including connection quality, tissue health, and polarization at the connections, significantly affect the V_{oc} value, especially when cells are connected in parallel. Research on Aloe cells and related reviews indicate that the reproducibility of results is partially dependent on the local state of the tissue and the conditions under which measurements are taken [8, 11].

F. Seven-day Visual Observation and Practical Implications

Clear signs of change are observable at the points of contact between the inserts and the plant. The leaf insertion demonstrates a more pronounced effect, evidenced by superior staining and drying outcomes at the puncture point. In contrast, the stem insertion exhibits a milder response, as illustrated in Fig. 12. This correlates with findings from previous experiments on aloe and its related varieties, indicating that such insertion may lead to a decline in output over time [11]. Durability serves as a critical aspect in evaluating the potential of ongoing features in plant harvesting, despite optimistic forecasts concerning voltage and current limitations [8].

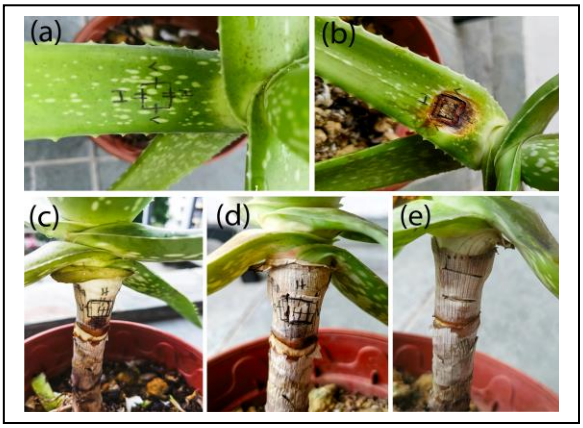

Fig. 12. Seven-day visual condition of insertion sites in *Aloe vera*: (a) Leaf day 0, (b) Leaf day 7, (c) Stem day 0, (d) Stem-V day 7 and (e) Stem-H day 7.

This study does not provide a multi-day electrical series. Photographs function as evidence in this context. The findings indicate that, despite the absence of guaranteed stability, satisfactory output from the stem and leaf at specific points correlates with enhanced stability relative to series and parallel wiring configurations. [8, 10, 11].

IV. CONCLUSION

This work presents a comparison of leaf and stem position, stem orientation, and simple series-parallel scaling in a *Zn-Cu* plant-based cell in *Aloe vera*. The horizontal arrangement of the leaf and stem produced comparable values of V_{oc} (0.958 V and 0.943 V) and similar I_{sc} values (0.15 mA and 0.12 mA). Stem orientation and electrode alignment were important factors influencing the current output. The vertical one produced a similar voltage of 0.904 V, but a much smaller current of 0.04 mA was obtained, which caused an increase in the calculated effective resistance. The leaf horizontal cell and a stem horizontal cell in series and in parallel produced 1.883 V and 0.25 mA, respectively, in agreement with the expected scaling. The equivalent-source perspective utilizing $R_{eff} = V_{oc}/I_{sc}$ provided a clear understanding of these results and supported the observed scaling behaviour. The 7-day photographs indicated a fracture at the leaf insertion site, while the stem site exhibited minimal disintegration. This suggests that the electric output associated with a plant stem can be comparable to that of a direct leaf placement, with the latter demonstrating superior visual longevity.

ACKNOWLEDGEMENT

The authors would like to acknowledge the Faculty of Artificial Intelligence and Engineering (FAIE) and Multimedia University (MMU) for supporting this research project.

FUNDING STATEMENT

The authors received no funding from any party for the research and publication of this article.

AUTHOR CONTRIBUTIONS

Sk Rakibur Rahman: Investigation, Methodology, Software, Data Curation, Formal Analysis, Writing–Original Draft

Ngu Eng Eng: Conceptualization, Investigation, Methodology, Formal Analysis, Validating, Writing–Review & Editing, Supervision, Project Administration.

Gwo-Chin Chung: Visualization, Validating, Writing–Review & Editing

Wai-Leong Pang: Visualization, Validating, Writing–Review & Editing

Kar-Ban Tan: Visualization, Validating, Writing–Review & Editing

Muhammad Aqeel Ashraf: Visualization, Validating, Writing–Review & Editing

Ajay Kumar Singh: Visualization, Validating, Writing–Review & Editing

Kah-Yoong Chan: Conceptualization, Investigation, Methodology, Formal Analysis, Validating, Writing–Review & Editing, Resources, Supervision, Project Administration.

CONFLICT OF INTERESTS

No conflict of interests was disclosed.

ETHICS STATEMENTS

The authors declare that this research did not involve human participants or animal subjects, and all work was conducted in accordance with the highest standards of research integrity and academic honesty.

DATA AVAILABILITY STATEMENT

The data are available from the corresponding author upon request.

REFERENCES

[1] F. K. Shaikh and S. Zeadally, "Energy Harvesting in Wireless Sensor Networks: A Comprehensive Review," *Renew. and Sustain. Ener. Rev.*, vol. 55, pp. 1041–1054, 2016.

[2] J. Y. Tan and K. Y. Chan, "Solar-based Nighttime Electric Power Generator Based on Radiative Cooling," *Ener. Rep.*, vol. 12, pp. 5155–5162, 2024.

[3] C. Ivana, M. Galina, I. Bukhori and T. Kurniawan, "The Application of Hybrid Renewable Energy Systems," *Int. J. Robot. Autom. Sci.*, vol. 7, no. 3, pp. 97–100, 2025.

[4] M. T. Sarker, M. H. S. M. Haram, G. Ramasamy, F. A. Farid and S. Mansor, "Solar Photovoltaic Home Systems in Malaysia: A Comprehensive Review and Analysis," *Energies*, vol. 16, no. 23, pp. 7718, 2023.

[5] F. T. Kabutey *et al.*, "An Overview of Plant Microbial Fuel Cells (PMFCs): Configurations and Applications," *Renew. and Sustain. Ener. Rev.*, vol. 110, pp. 402–414, 2019.

[6] R. Nitisoravut and R. Regmi, "Plant Microbial Fuel Cells: A Promising Biosystems Engineering," *Renew. and Sustain. Ener. Rev.*, vol. 76, pp. 81–89, 2017.

[7] P. Bombelli *et al.*, "Electrical Output of Bryophyte Microbial Fuel Cell Systems is Sufficient to Power A Radio or An Environmental Sensor," *Royal Soc. Open Sci.*, vol. 3, no. 10, pp. 160249, 2016.

[8] S. R. Rahman *et al.*, "Energy Harvesting from Living Plant: A Review on Past Research and Way Forward," *Ener. Rep.*, vol. 14, pp. 268–281, 2025.

[9] Y. Y. Choo, J. Dayou and N. Surugau, "Origin of Weak Electrical Energy Production from Living-Plants," *Int. J. Renew. Ener. Res.*, vol. 4, no. 1, pp. 198–203, 2014.

[10] P. L. Chong, A. K. Singh and S. L. Kok, "Potential Application of Aloe Vera-Derived Plant-Based Cell in Powering Wireless Device for Remote Sensor Activation," *PLoS One*, vol. 14, no. 12, pp. e0227153, 2019.

[11] P. L. Chong, A. K. Singh and S. L. Kok, "Characterization of Aloe Barbadensis Miller Leaves as A Potential Electrical Energy Source with Optimum Experimental Setup Conditions," *PLoS One*, vol. 14, no. 6, pp. e0218758, 2018.

[12] W. Apollon *et al.*, "Impact of Opuntia Species Plant Bio-Battery in A Semi-Arid Environment: Demonstration of Their Applications," *Appl. Ener.*, vol. 279, pp. 115788, 2020.

[13] F. Meder *et al.*, "Energy Conversion at The Cuticle of Living Plants," *Adv. Funct. Mater.*, vol. 28, no. 51, pp. 1806689, 2018.

[14] V. Flexer and N. Mano, "From Dynamic Measurements of Photosynthesis in A Living Plant to Sunlight Transformation into Electricity," *Analyt. Chem.*, vol. 82, no. 4, pp. 1444–1449, 2010.

[15] S. R. Rahman *et al.*, "Energy Harvesting from Plants using Plant-Based Cells," in *2025 Multimedia Univ. Eng. Conf.*, Cyberjaya, pp. 1–6, pp.11277229, 2025.

[16] S. R. Rahman *et al.*, "Biocompatible Graphite-Coated Electrodes for Sustainable Plant-Based Energy Harvesting," *Geol., Ecol., and Landsc.*, pp. 1–12, pp. 2640713, 2026.

[17] S. R. Rahman *et al.*, "Electrode-Leaf Interface Optimization for Maximizing Plant Bioelectrical Energy Harvesting," in *2026 Multimedia Univ. Eng. Conf.*, Cyberjaya, pp. 1–6, 2026.